International Journal of Thermophysics, Vol. 26, No. 2, March 2005 (© 2005)
DOI: 10.1007/s10765-005-4510-0

Multiphase Equation of State for Carbon over Wide Range of Temperatures and Pressures[1]

K. V. Khishchenko,[2,3] V. E. Fortov,[2] and I. V. Lomonosov[4]

A semiempirical equation-of-state model, which takes into account the effects of polymorphic phase transformation and melting, is proposed. An equation of state is developed for graphite, diamond, and liquid phases of carbon, and a critical analysis of calculated results in comparison with available high-temperature, high-pressure experimental data is made.

KEY WORDS: diamond; equation of state; graphite; liquid carbon; phase diagram; shock Hugoniot.

1. INTRODUCTION

A knowledge of the thermodynamic properties and phase changes of matter in a wide region of states diagram is of fundamental as well as practical interest [1]. The multi-phase equation of state (EOS) of carbon over the range from normal conditions to extremely high values of temperature and pressure is required for numerical simulation of hydrodynamic processes under conditions of high energy densities [1–3].

We propose a new semiempirical EOS model, which takes into account the polymorphic phase transformation and melting effects. A wide-range EOS for graphite–diamond–liquid carbon system is constructed on the basis of the model developed. Calculated results are compared

[1]Paper presented at the Sixteenth European Conference on Thermophysical Properties, September 1–4, 2002, London, United Kingdom.

[2]Institute for High Energy Densities, Russian Academy of Sciences, Izhorskaya 13/19, Moscow 125412, Russia.
[3]To whom correspondence should be addressed. E-mail: konst@ihed.ras.ru
[4]Institute of Problems of Chemical Physics, Russian Academy of Sciences, Chernogolovka 142432, Russia.

with available experimental data in a broad region of the phase diagram. The most essential shock-loading and adiabatic-release experiments are described.

2. EOS MODEL

According to the EOS model, the Helmholtz free energy for matter is considered as a sum of three components,

$$F(V,T) = F_c(V) + F_a(V,T) + F_e(V,T), \tag{1}$$

describing the elastic part of the interaction at $T = 0\,\mathrm{K}$ (F_c) and the thermal contributions by atoms (F_a) and electrons (F_e). The first and third components in Eq. (1) have a different form for graphite and diamond, but the second is defined by identical functional relationships for both solid phases of carbon. The free energy F of liquid carbon has the form of Eq. (1) with the same expressions for terms as the thermodynamic potential of the liquid phase in the EOS model [1].

The elastic component of energy for the diamond phase in the compression region ($\sigma_c \geqslant 1$, where $\sigma_c = V_{0c}/V$, V_{0c} is specific volume at $P = 0$, $T = 0\,\mathrm{K}$) is given in the form [4],

$$F_c(V) = E_{0c} + 3V_{0c}\sum_{i=1}^{6}\frac{a_i}{i}\left(\sigma_c^{i/3} - 1\right), \tag{2}$$

providing for the condition

$$F_c(V_{0c}) = E_{0c}. \tag{3}$$

Also, the following additional conditions must be satisfied along the cold compression curve at $\sigma_c = 1$:

$$P_c(V_{0c}) = -dF_c/dV = 0, \tag{4}$$

$$B_c(V_{0c}) = -V\,dP_c/dV = B_{0c}, \tag{5}$$

$$B_c'(V_{0c}) = dB_c/dP_c = B_{0c}', \tag{6}$$

where P_c is the pressure, B_c is the bulk modulus, and B_c' is its pressure derivative. Equations (4)–(6) are complemented by the requirement of a minimal root-mean-square deviation of the pressure in the range $\sigma_c = 30$–1000 from calculated values of P_c^{TFC} obtained using the Thomas–Fermi

model with quantum and exchange corrections [5]. This results in the problem of finding a conditional extremum of the functional,

$$S(a_i, \lambda, \mu, \eta) = \sum_{n=1}^{N} g_n \left[1 - P_c(a_i, V_n)/P_c^{TFC}(V_n)\right]^2 + \lambda P_c(a_i, V_{0c}) + \mu [B_c(a_i, V_{0c}) - B_{0c}] + \eta \left[B'_c(a_i, V_{0c}) - B'_{0c}\right], \quad (7)$$

the solution of which gives the value for the coefficients a_i. The values of parameters V_{0c}, B_{0c}, and B'_{0c} are chosen by means of iterations so that the value of the specific volume, $V = V_0$, and the isentropic bulk modulus,

$$B_S = -V \left(\partial P / \partial V\right)_S = B_{S0}, \quad (8)$$

and its derivative with respect to pressure,

$$B'_S = \left(\partial B_S / \partial P\right)_S = B'_{S0}, \quad (9)$$

determined from the results of dynamic measurements, would be satisfied under normal conditions, $P = 0.1$ MPa and $T = 293$ K.

The cold energy of the diamond phase in the rarefaction region ($\sigma_c < 1$) is represented by a polynomial of the form,

$$F_c(V) = V_{0c} \left[a_m \left(\sigma_c^m/m - \sigma_c^l/l\right) + a_n \left(\sigma_c^n/n - \sigma_c^l/l\right)\right] + E_{sub}, \quad (10)$$

which leads to the correct value of the sublimation energy E_{sub} in the case of $V \to \infty$ [6] and satisfies Eq. (4). Equations (3), (5), and (6) leave two fitting parameters, n and l, in Eq. (10).

The volume dependence of the elastic component of energy for the graphite phase over a whole range of compression ratio, σ_c, is expressed in the form of Eq. (10) simplified in such a way that $l = n$ while taking into account Eq. (5):

$$F_c(V) = \frac{B_{0c} V_{0c}}{m - n} \left(\sigma_c^m/m - \sigma_c^n/n\right) + E_{sub}. \quad (11)$$

In this case, normalizing Eq. (3) with $E_{0c} = 0$ gives $n = B_{0c} V_{0c} (m E_{sub})^{-1}$, and the requirement of Eq. (6) determines the relation $m = B'_{0c} - n - 2$. Therefore, a choice of values of V_{0c}, B_{0c}, and B'_{0c} defines all parameters in Eq. (11).

The lattice contribution to the free energy of the solid phases is defined by excitation of acoustic and optical modes of thermal vibrations of atoms:

$$F_{\mathrm{a}}(V,T)=F_{\mathrm{a}}^{\mathrm{acst}}(V,T)+\sum_{\alpha=1}^{3(\nu-1)}F_{\mathrm{a}\alpha}^{\mathrm{opt}}(V,T), \tag{12}$$

$$F_{\mathrm{a}}^{\mathrm{acst}}(V,T)=\frac{RT}{\nu}\left[3\ln\left(1-e^{-\theta^{\mathrm{acst}}/T}\right)-D(\theta^{\mathrm{acst}}/T)\right]-\beta_{\mathrm{acst}}\frac{T^2/\theta^{\mathrm{acst}}}{e^{\theta^{\mathrm{acst}}/T}-1}, \tag{13}$$

$$F_{\mathrm{a}\alpha}^{\mathrm{opt}}(V,T)=\frac{RT}{\nu}\ln\left(1-e^{-\theta_\alpha^{\mathrm{opt}}/T}\right)-\beta_{\mathrm{opt}\alpha}\frac{T^2/\theta_\alpha^{\mathrm{opt}}}{e^{\theta_\alpha^{\mathrm{opt}}/T}-1}, \tag{14}$$

where R is the gas constant, ν is the number of atoms in an elementary cell of the lattice, D is the Debye function [7],

$$D(x)=\frac{3}{x^3}\int_0^x\frac{t^3dt}{e^t-1}, \tag{15}$$

and θ^{acst} and $\theta_\alpha^{\mathrm{opt}}$ are the characteristic temperatures of the acoustic and optical modes of phonon spectrum [8, 9],

$$\begin{aligned}\theta^{\mathrm{acst}}(V)/\theta_0^{\mathrm{acst}}&=\theta_\alpha^{\mathrm{opt}}(V)/\theta_{0\alpha}^{\mathrm{opt}}\\&=\sigma^{2/3}\exp\left\{(\gamma_0-2/3)\frac{\sigma_n^2+\ln^2\sigma_m}{\sigma_n}\mathrm{arctg}\left[\frac{\sigma_n\ln\sigma}{\sigma_n^2-\ln(\sigma/\sigma_m)\ln\sigma_m}\right]\right\},\end{aligned} \tag{16}$$

where $x=\ln\sigma$, $\sigma=V_0/V$, γ_0 is the value of the Grüneisen coefficient under normal conditions, and σ_m and σ_n are free parameters, chosen from the requirement of the optimum description of experimental data on thermal expansion of studied substances [10]. The values of coefficients θ_0^{acst} and $\theta_{0\alpha}^{\mathrm{opt}}$ are defined from measured values of the isobaric heat capacity C_P of graphite and diamond at normal pressure and various temperatures [11, 12].

The last terms in Eqs. (13) and (14) take into account the effects of anharmonicity of thermal lattice vibrations. These terms are exponentially small at low temperatures and provide for behavior of heat capacity, $C_V-3R\sim T^2$ at $T\to\infty$ [11]. The requirement that the contributions of anharmonicity terms for all acoustic and optical vibrations modes at $T\to\infty$ are equal to each other lets us introduce a coefficient ξ_{a}, such that

$$\beta_{\mathrm{acst}}=3\xi_{\mathrm{a}}\theta_0^{\mathrm{acst}^2}/\nu,\quad \beta_{\mathrm{opt}\alpha}=\xi_{\mathrm{a}}\theta_{0\alpha}^{\mathrm{opt}^2}/\nu. \tag{17}$$

The value of ξ_{a} for graphite is found from high-temperature data for enthalpy under normal pressure [13]. The value of ξ_{a} for diamond is

determined from experimental data on the equilibrium boundary between graphite and diamond [14–17].

The electron contribution to the free energy of diamond, which is a dielectric with the energy gap between the valence and conduction bands $\Delta_0 \simeq 5.5\,\text{eV}$ [18], is negligible in comparison with F_a at temperatures $T \ll \Delta_0/2k$ (where k is the Boltzmann constant). Therefore,

$$F_e(V, T) = 0 \tag{18}$$

for the diamond phase.

The electronic component of the free energy of the graphite phase is given by the expression,

$$F_e(V, T) = -\frac{1}{2}\beta_0 T^2 \sigma^{-\gamma_0}, \tag{19}$$

where β_0 is the coefficient of electronic heat capacity at $T = 0\,\text{K}$ [11].

The coefficients of EOS that optimally generalize the available experimental and theoretical data for diamond within the framework of Eqs. (1), (2), (10), and (12)–(18) are as follows: $V_0 = 0.2845$, $V_{0c} = 0.28443$, $E_{0c} = 0.31$, $a_1 = -153.381$, $a_2 = -1486.526$, $a_3 = 2161.515$, $a_4 = -591.265$, $a_5 = 72.861$, $a_6 = -3.204$, $a_m = 329.218$, $a_n = -23.108$, $m = 2.9164$, $n = 9$, $l = 1$, $E_{sub} = 56$, $\nu = 8$, $R = 0.69224$, $\theta_0^{acst} = 1.1$, $\theta_{0\alpha}^{opt} = 1.49$, $\xi_a = 0.00088$, $\gamma_0 = 0.9$, $\sigma_m = 0.855$, and $\sigma_n = 0.1$.

The coefficients in Eqs. (1), (11)–(17), and (19) providing an optimum description of the available thermodynamic information for graphite are as follows: $V_0 = 0.4415$, $V_{0c} = 0.44102$, $B_{0c} = 35.597$, $m = 7.238$, $n = 0.039$, $E_{sub} = 56$, $\nu = 2$, $R = 0.69224$, $\theta_0^{acst} = 1.05$, $\theta_{0\alpha}^{opt} = 1.8$, $\xi_a = 0.001$, $\gamma_0 = 0.243$, $\sigma_m = 0.6$, $\sigma_n = 1$, and $\beta_0 = 0.00117$.

The units of measurement for the listed coefficients correspond to the original units $E = 1\,\text{kJ}\cdot\text{g}^{-1}$, $V = 1\,\text{cm}^3\cdot\text{g}^{-1}$, and $T = 1\,\text{kK}$.

3. THERMODYNAMIC PROPERTIES OF CARBON

The compressibility of graphite at normal temperature was investigated experimentally in X-ray diffraction measurements using supported anvils [19] and diamond-anvil cells [20, 21] in combination with different pressure scales up to $P \simeq 20\,\text{GPa}$. Calculated isotherm of $T = 293\,\text{K}$ for graphite in comparison with experimental data from Refs. 19–21 is presented in Fig. 1. Shock-wave point from Ref. 23, which corresponds to maximum compression of highly oriented graphite before its fast transformation to diamond, is also shown in Fig. 1.

The adequacy of the proposed form of contribution of thermal lattice vibrations to the thermodynamic potential is illustrated in Fig. 2, in which

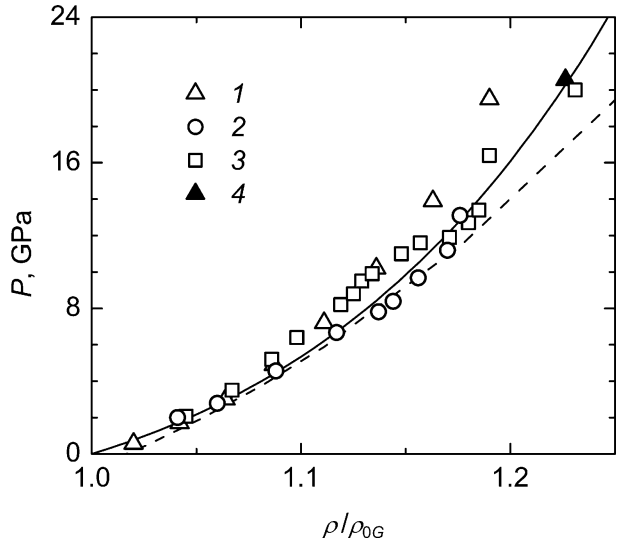

Fig. 1. Pressure versus relative compression of graphite at $T = 293\,\mathrm{K}$. Solid line corresponds to this work; dashed line is calculated isotherm $T = 0\,\mathrm{K}$ from Ref. 22; $\rho_{0G} = 2.265\,\mathrm{g \cdot cm^{-3}}$. Experimental data: 1, Ref. 19; 2, Ref. 20; 3, Ref. 21; 4, Ref. 23.

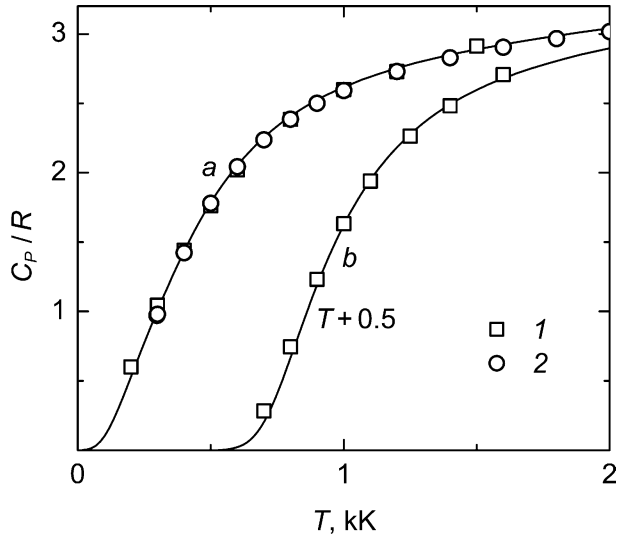

Fig. 2. Isobaric heat capacity versus temperature of graphite (a) and diamond (b) under atmospheric pressure, $R = 0.69224\,\mathrm{J \cdot g^{-1} \cdot K^{-1}}$. Experimental data: 1, Ref. 11; 2, Ref. 12.

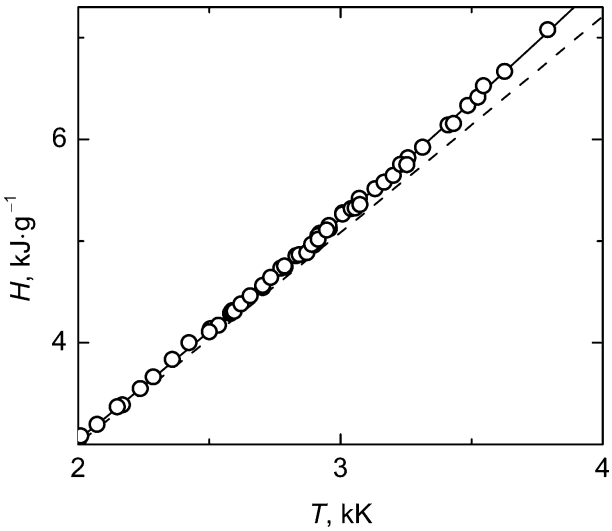

Fig. 3. Specific enthalpy versus temperature of graphite under atmospheric pressure. Solid line corresponds to calculations taking into account the anharmonicity effects; dashed line denotes results without these effects; open circles represent experimental data from Ref. 13.

the calculated values of the isobaric heat capacity of graphite and diamond at normal pressure and moderate temperatures are compared with experimental data [11, 12]. Results of enthalpy calculations for graphite in comparison with high-temperature data from Ref. 13 are presented in Fig. 3. The atmospheric isobar of graphite enthalpy calculated with $\xi_a = 0$ in Eq. (17) is shown in Fig. 3 to demonstrate the influence of the anharmonicity effects on the EOS of solid carbon at high temperatures.

Thermodynamic properties and phase changes of graphite and diamond at high pressures and temperatures are investigated in dynamic experiments in detail.

Methods of shock and adiabatic release waves diagnostics are based on the use of the relationship between the thermophysical properties of the medium under study and the hydrodynamic characteristics of the flow of matter observed experimentally [24]. Traditionally, one attempts to use self-similar solutions of a stationary shock-wave type and of centered Riemann-expansion-wave type describing the conservation laws in a simple algebraic or integrals form [25]. At a stationary shock discontinuity passing through a substance, the laws of conservation of mass, momentum, and energy must be satisfied in the shock-wave front [24]:

$$V = V_{00}\frac{U_s - U_p}{U_s}, \tag{20}$$

$$P = P_0 + \frac{U_s U_p}{V_{00}}, \tag{21}$$

$$E = E_0 + \frac{1}{2}(P_0 + P)(V_{00} - V), \tag{22}$$

where V_{00} is initial specific volume of sample, P_0 and E_0 are initial values of pressure and specific internal energy, U_s and U_p are shock and particle velocities, and V, P, and E are specific volume, pressure, and specific internal energy, respectively, behind the shock-wave front. The energy conservation law, Eq. (22), is the well known Hugoniot equation [24]. In the experiments for the determination of the isentropic expansion curve of a shock-compressed substance with V_H, P_H, and E_H, the corresponding states in an expansion wave are described by the Riemann integrals [24],

$$V = V_H + \int_P^{P_H} \left(dU_p/dP\right)^2 dP, \tag{23}$$

$$E = E_H - \int_P^{P_H} P\left(dU_p/dP\right)^2 dP, \tag{24}$$

taken along the measured isentrope $P = P(U_p)$.

Using the EOS, for example, in a thermodynamically complete form,

$$P = -(\partial F/\partial V)_T = P(V, T) \text{ and } E = F - T(\partial F/\partial T)_V = E(V, T), \tag{25}$$

lets one to calculate the characteristics of matter in waves of shock compression and adiabatic release. For experiments under initial conditions of $P_0 = 0.1$ MPa and $T_0 = 293$ K, the initial volume of sample is varied: $V_{00} = V_0$, in a case of solid samples, and $V_{00} > V_0$, in a case of porous samples; $E_0 = E(V_0, T_0)$, for any value of V_{00} [24]. Taking into account these initial parameters, Eqs. (22) and (25) define a relationship of $V(P)$ and $T(P)$ for shock-compressed sample. The hydrodynamic characteristics are obtained from Eqs. (20) and (21),

$$U_s = V_{00}\sqrt{\frac{P - P_0}{V_{00} - V}}, \tag{26}$$

$$U_p = \sqrt{(P - P_0)(V_{00} - V)}. \tag{27}$$

For experiments with reflected shock waves, the initial parameters V_{00}, P_0, and E_0 in Eqs. (20)–(22) correspond to states of matter behind the first

shock wave [25]. For experiments with adiabatic release waves, the thermodynamic parameters of substance are defined by the condition,

$$S = -(\partial F/\partial T)_V = \text{const}, \tag{28}$$

and an increase of particle velocity is calculated from the integral,

$$U_\text{p} = U_\text{H} + \int_{V_\text{H}}^{V} (-\partial P/\partial V)_\text{S}^{1/2}\, dV, \tag{29}$$

where U_H corresponds to initial velocity of flow behind the front of the first shock-compression wave.

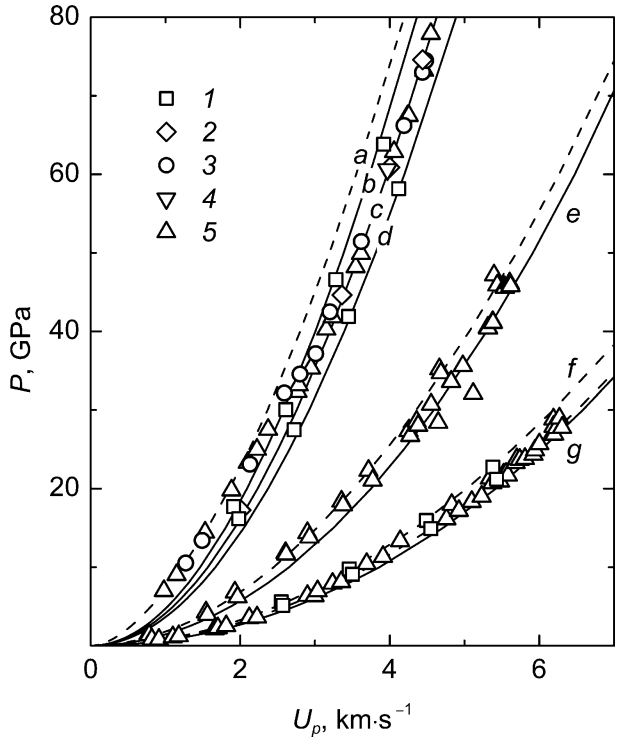

Fig. 4. Shock Hugoniots, plotted as pressure versus particle velocity, of diamond and graphite samples with initial densities $\rho_{00} = 1.87$ (a, c), 2.02 (b), 1.789 (d), 1.011 (e), 0.607 (f), and $0.56\,\text{g}\cdot\text{cm}^{-3}$ (g). Solid and dashed lines denote results of calculation for diamond and graphite, respectively. Experimental data for diamond (1, 2) and graphite (3–5) samples: 1 and 3, Ref. 26; 2, Ref. 27; 4, Refs. 29 and 30; 5, Ref. 31.

As follows from Figs. 4 to 6, the multi-phase EOS constructed for carbon adequately describes the experimental data for graphite and diamond of different initial densities [23, 26–32] over the entire range of dynamic characteristics generated in shock-loading and adiabatic-release waves.

An analysis of the results of measurements of sound velocity in shock compressed graphite with initial density $\rho_{00} = V_{00}^{-1} = 2.2\,\mathrm{g \cdot cm^{-3}}$ [33] indicates that carbon is in the solid diamond phase at pressures in the range 80–143 GPa. On the calculated shock Hugoniot of graphite with $\rho_{00} = 2.2\,\mathrm{g \cdot cm^{-3}}$, melting of diamond begins at $P \simeq 150$ GPa; this value is consistent with experimental data [33].

The phase diagram of carbon calculated on the basis of the developed EOS is shown in Fig. 7. It reveals a region of states realized in the

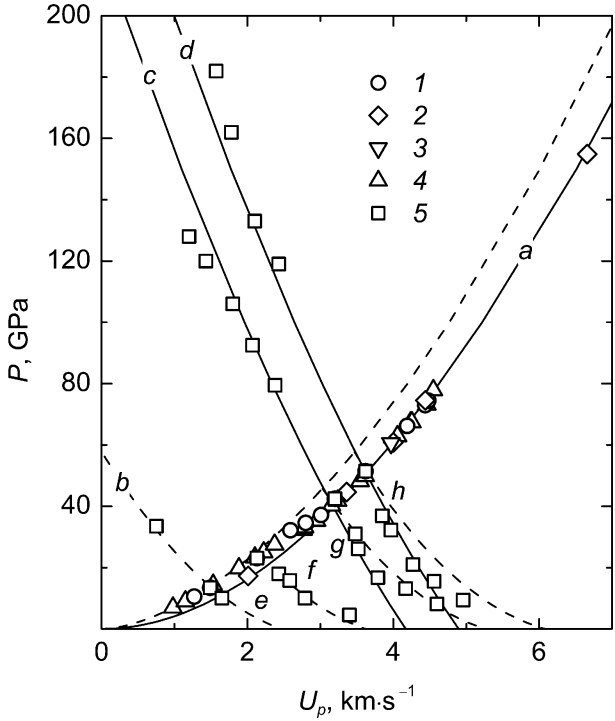

Fig. 5. Shock Hugoniot (a), curves of second shock compression (b–d), and release isentropes (e–h), plotted as pressure versus particle velocity, of graphite samples with initial density $\rho_{00} = 1.87\,\mathrm{g \cdot cm^{-3}}$. Solid and dashed lines denote results of calculation for diamond and graphite, respectively. Data from experiments with direct shock (1–4) and reflected shock and release (5) waves: 1 and 5, Ref. 26; 2, Ref. 27; 3, Refs. 29 and 30; 4, Ref. 31.

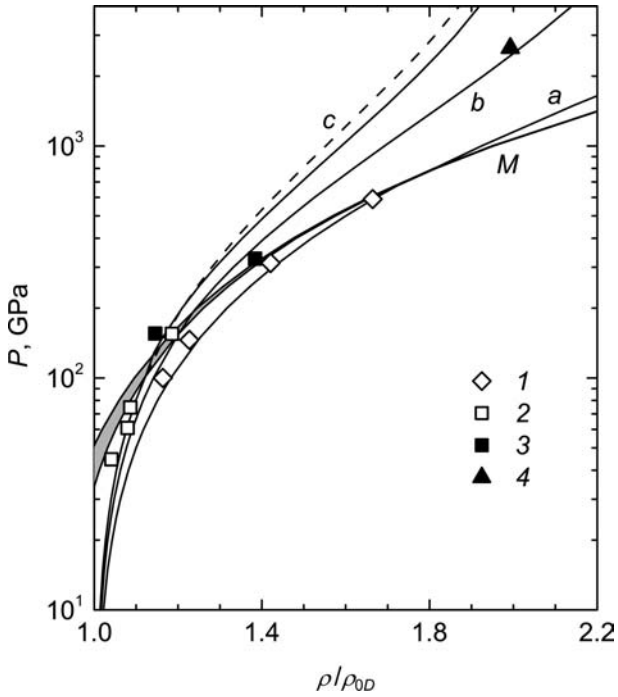

Fig. 6. Pressure versus relative compression of carbon at high pressures. *M* is diamond melting region; (a)–(c) are shock Hugoniots of carbon samples with initial densities $\rho_{00} = 3.51$ (a), 2.235 (b), and $1.9\,\mathrm{g \cdot cm^{-3}}$ (c); $\rho_{0D} = 3.515\,\mathrm{g \cdot cm^{-3}}$. Solid lines denote results of calculation with taking into account the melting effects; dashed line corresponds to metastable diamond. Experimental data from measurements with diamond (1, 2) and graphite (3, 4) samples: 1 and 2, $\rho_{00} = 3.51$ and $1.9\,\mathrm{g \cdot cm^{-3}}$, respectively, Ref. 27; 3, $\rho_{00} = 1.85\,\mathrm{g \cdot cm^{-3}}$, Ref. 28; 4, $\rho_{00} = 2.235\,\mathrm{g \cdot cm^{-3}}$, Ref. 32.

dynamic experiments with traditional explosives systems [26, 27, 31] and a two-stage light-gas gun [33]. As can be seen, these shock-wave data correspond to both solid and liquid phases of carbon.

4. CONCLUSION

The multi-phase EOS we have developed for carbon provides a consistent representation of the available experimental data, and it can be employed effectively in numerical simulation of hydrodynamic processes at high energy densities.

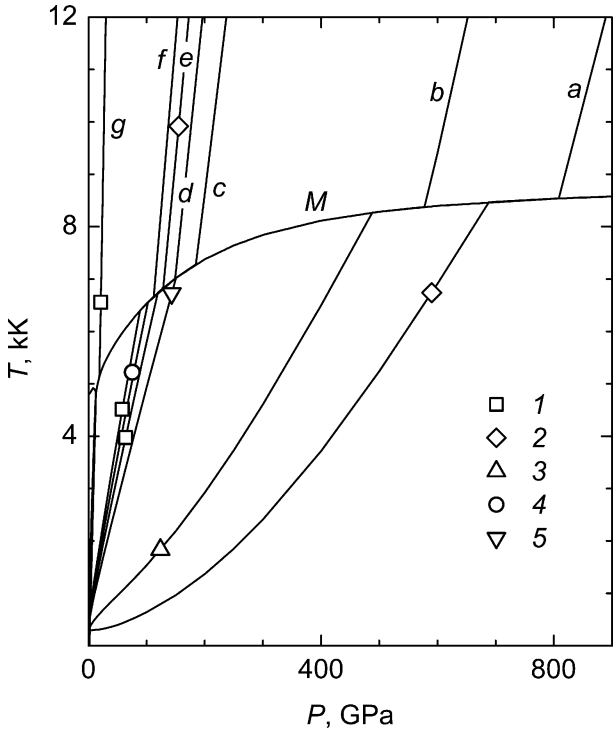

Fig. 7. Phase diagram of carbon. *M* is diamond melting curve; (a)–(g) are shock Hugoniots of carbon samples with initial densities $\rho_{00} = 3.51$ (a), 3.191 (b), 2.2 (c), 2.02 (d), 1.87 (e), 1.789 (f), and $0.56\,\mathrm{g \cdot cm^{-3}}$ (g). The level of pressures realized in experiments with diamond (1–3) and graphite (4, 5) samples: 1 and 4, Ref. 26; 2, Ref. 27; 3, Ref. 31; 5, Ref. 33.

ACKNOWLEDGMENTS

The work was carried out under financial support of the Russian Foundation for Basic Research, Grant 03-02-16687.

REFERENCES

1. A. V. Bushman, V. E. Fortov, G. I. Kanel', and A. L. Ni, *Intense Dynamic Loading of Condensed Matter* (Taylor & Francis, Washington, 1993).
2. A. V. Bushman, V. S. Vorob'ev, V. N. Korobenko, A. D. Rakhel, A. I. Savvatimskii, and V. E. Fortov, *Int. J. Thermophys.* **14:**565 (1993).
3. I. V. Lomonosov, V. E. Fortov, A. A. Frolova, K. V. Khishchenko, A. A. Charakhch'yan, and L. V. Shurshalov, *Phys. Dokl.* **43:**306 (1998).

4. A. V. Bushman, I. V. Lomonosov, and V. E. Fortov, *Sov. Tech. Rev. B. Therm. Phys.* **5:**1 (1993).
5. N. N. Kalitkin and L. V. Kuz'mina, *Tables of Thermodynamic Functions of Matter at High Energy Concentration*, Preprint Inst. Prikl. Matem. Akad. Nauk SSSR No. 35 (Institute of Applied Mathematics, USSR Academy of Sciences, Moscow, 1975).
6. R. Hultgren, P. D. Desai, D. T., Hawkins, M. Gleiser, K. K. Kelley, and D. D. Wagman, *Selected Values of the Thermodynamic Properties of the Elements* (ASME, Metals Park, Ohio, 1973).
7. L. D. Landau and E. M. Lifshitz, *Statistical Physics* (Pergamon Press, Oxford, 1980).
8. K. V. Khishchenko, I. V. Lomonosov, and V. E. Fortov, *High Temp.-High Press.* **30:**373 (1998).
9. K. V. Khishchenko, V. E. Fortov, and I. V. Lomonosov, *Int. J. Thermophys.* **23:**211 (2002).
10. Y. S. Touloukian, R. K. Kirby, R. E. Taylor, and T. Y. R. Lee, *Thermophysical Properties of Matter, TPRC Data Series*, Vol. 13, *Thermal Expansion. Nonmetallic Solids* (IFI/Plenum, New York, 1977), p. 16.
11. B. Wunderlich and H. Baur, *Fortschritte Hochpolym. Forschung* **7:**151 (1970).
12. G. A. Bergman, L. M. Buchnev, I. I. Petrova, V. N. Senchenko, L. R. Fokin, V. Ya. Chekhovskoi, and M. A. Sheindlin, *Tables of Standard Reference Data. GSSSD 25–90* (Izdatel'stvo Standartov, Moscow, 1991).
13. L. M. Buchnev, A. I. Smyslov, I. A. Dmitriev, A. F. Kuteinikov, and V. I. Kostikov, *Dokl. Akad. Nauk SSSR* **278:**1109 (1984).
14. F. P. Bundy, H. P. Bovenkerk, H. M. Strong, and R. H. Wentorf, Jr., *J. Chem. Phys.* **35:**383 (1961).
15. H. M. Strong and R. E. Hanneman, *J. Chem. Phys.* **46:**3668 (1967).
16. H. M. Strong and R. M. Chrenko, *J. Phys. Chem.* **75:**1838 (1971).
17. C. S. Kennedy and G. C. Kennedy, *J. Geophys. Res.* **81:**2467 (1976).
18. S. Fahy and S. G. Louie, *Phys. Rev. B* **36:**3373 (1987).
19. R. W. Lynch and H. G. Drickamer, *J. Chem. Phys.* **44:**181 (1966).
20. M. Hanfland, H. Beister, and K. Syassen, *Phys. Rev. B* **39:**12598 (1989).
21. Y. X. Zhao and I. L. Spain, *Phys. Rev. B* **40:**993 (1989).
22. J. C. Boettger, *Phys. Rev. B* **55:**11202 (1997).
23. D. J. Erskine and W. J. Nellis, *J. Appl. Phys.* **71:**4882 (1992).
24. Ya. B. Zel'dovich and Yu. P. Raizer, *Physics of Shock Waves and High-Temperature Hydrodynamic Phenomena* (Academic Press, New York, 1967).
25. L. V. Al'tshuler, *Sov. Phys. Usp.* **8:**52 (1965).
26. K. V. Khishchenko, V. E. Fortov, I. V. Lomonosov, M. N. Pavlovskii, G. V. Simakov, and M. V. Zhernokletov, in *Shock Compression of Condensed Matter – 2001*, M. D. Furnish, N. N. Thadhani, and Y. Horie, eds. (AIP, Melville, New York, 2002), p. 759.
27. M. N. Pavlovskii, *Sov. Phys. Solid State* **13:**741 (1971).
28. M. N. Pavlovskii and V. P. Drakin, *JETP Lett.* **4:**116 (1966).
29. R. F. Trunin, G. V. Simakov, B. N. Moiseev, L. V. Popov, and M. A. Podurets, *Sov. Phys. JETP* **29:**628 (1969).
30. R. F. Trunin, *Phys. Usp.* **37:**1123 (1994).
31. S. P. Marsh, ed., *LASL Shock Hugoniot Data* (University of California Press, Berkeley, 1980).
32. C. E. Ragan III, *Phys. Rev. A* **29:**1391 (1984).
33. J. W. Shaner, J. M. Brown, C. A. Swenson, and R. G. McQueen, *J. de Phys.* **45:**C8–235 (1984).